

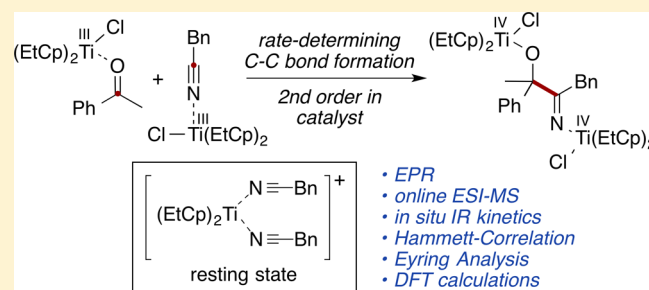
Mechanism of the Ti^{III}-Catalyzed Acyloin-Type Umpolung: A Catalyst-Controlled Radical Reaction

Jan Streuff,^{*,†} Markus Feurer,[†] Georg Frey,[†] Alberto Steffani,[†] Sylwia Kacprzak,[‡] Jens Weweler,[†] Leonardus H. Leijendekker,[†] Daniel Kratzert,[§] and Dietmar A. Plattner[†]

[†]Institut für Organische Chemie, [‡]Institut für Physikalische Chemie, and [§]Institut für Anorganische und Analytische Chemie, Albert-Ludwigs-Universität Freiburg, Albertstr. 21, 79104 Freiburg, Germany

S Supporting Information

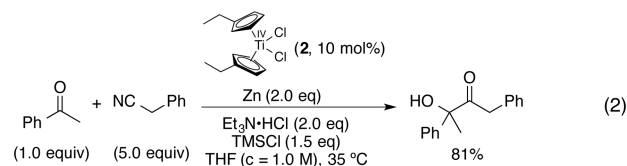
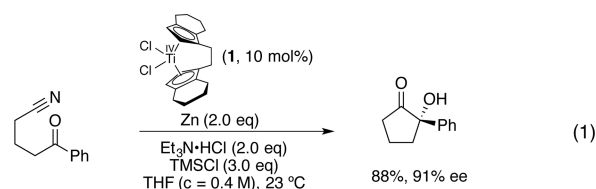
ABSTRACT: The titanium(III)-catalyzed cross-coupling between ketones and nitriles provides an efficient stereoselective synthesis of α -hydroxyketones. A detailed mechanistic investigation of this reaction is presented, which involves a combination of several methods such as EPR, ESI-MS, X-ray, in situ IR kinetics, and DFT calculations. Our findings reveal that C–C bond formation is turnover-limiting and occurs by a catalyst-controlled radical combination involving two titanium(III) species. The resting state is identified as a cationic titanocene-nitrile complex and the beneficial effect of added Et₃N·HCl on yield and enantioselectivity is elucidated: chloride coordination initiates the radical coupling. The results are fundamental for the understanding of titanium(III)-catalysis and of relevance for other metal-catalyzed radical reactions. Our conclusions might apply to a number of reductive coupling reactions for which conventional mechanisms were proposed before.



INTRODUCTION

The development of catalytic C–C bond forming reactions is one of the central topics of synthetic organic chemistry.¹ Over the past years, reductive cross-coupling reactions have gained increasing attention since they enable new connections under often mild reaction conditions starting from readily available substrates.² Among them are so-called reductive umpolung reactions that forge molecules with functionalization in even bond distances from two similarly polarized carbon fragments.^{3–5} Recently, transition metal catalyzed protocols have evolved that allow the control of the chemo- and stereoselectivity in such transformations.⁵ In particular, titanium(III) catalysis is superior for achieving high selectivity in pinacol couplings and related reactions.^{6–8} Importantly, these titanium(III) catalyzes are radical reactions that proceed under full catalyst control of stereo- regio- and chemoselectivity, which is a striking advantage over classical free radical reactions. However, the usually heterogeneous reaction mixtures and the presence of open-shell systems make them notoriously difficult to examine. In particular, the mechanism of the titanium(III)-catalyzed pinacol coupling has been subject of a longstanding debate.⁹

We recently advanced the concept of catalytic reductive umpolung toward cross-coupling reactions, for which only few examples existed in the literature.^{6,10,11} An asymmetric reductive radical cyclization of ketonitriles was developed that led to enantioenriched α -hydroxyketones in the presence of chiral *ansa*-titanocene **1** (eq 1).^{10e,12} The addition of Et₃N·HCl had a remarkable influence on the enantioselectivity, which was



unusual and deserved further investigation. Afterward, a more general cross-coupling with substituted titanocene **2** as catalyst was established, which enabled the modular synthesis of linear α -hydroxyketones from readily available precursors such as acetophenone (PhCOMe) and benzyl cyanide (BnCN) (eq 2).^{10c} To understand the features of this titanium(III)-catalyzed acyloin-type coupling, a mechanistic investigation was envisioned, but the previously faced difficulties had to be overcome. To this end, we applied a combined approach of EPR, online ESI-MS, in situ IR, and DFT investigations as well as stoichiometric experiments that allowed the examination of such difficult cases in unprecedented mechanistic detail. The

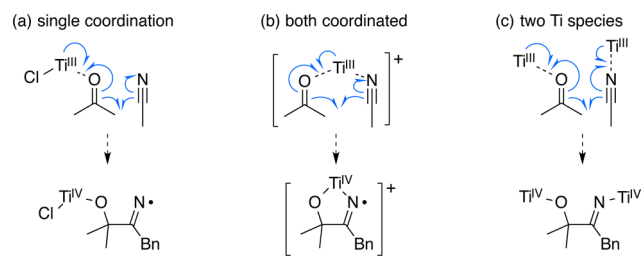
Received: August 31, 2015

Published: October 23, 2015

results gave valuable insight into the nature of titanium(III)-catalyzed C–C forming processes and could become relevant for radical reactions catalyzed by other metals as well.

In the past, several scenarios were proposed for titanium(III)-mediated or -catalyzed reductive umpolung reactions involving carbonyls.^{5,6} Hence, one of the key goals of this study was the elucidation of the nature of the central C–C bond forming event using the title reaction as example. The C–C coupling reaction shown in eq 2 could for example take place at a single titanium(III) center coordinating (a) only to the ketone^{12,13} or (b) coordinating ketone and nitrile, which would lead to the formation of either a neutral- or a cationic nitrogen-centered radical, respectively (Scheme 1).

Scheme 1. Selected Possible C–C Forming Pathways



Alternatively, a second titanium(III) species could coordinate to the nitrile, leading to a bimolecular pathway (c) via a radical combination, avoiding the formation of high-energy N-radical intermediates.^{10c,14} A Ti–N and Ti–O cleavage followed by imine hydrolysis during workup would then form the hydroxyketone product.

Before the discussion of the results of this study, it is important to note that the composition of the titanium(III) species in solution is strongly influenced by the reaction conditions: coordinating molecules such as acetonitrile or water solvate the chloride ligands leading to cationic titanium species.^{15–17} Reduction of Cp_2TiCl_2 with zinc dust in THF, on the other hand, leads to a mixture of a monomeric $[\text{Cp}_2\text{TiCl}]$ and its chloride bridged dimer $[(\text{Cp}_2\text{TiCl})_2]$ without the formation of cationic $[\text{Cp}_2\text{Ti}]^+$ or Zn-bridged dimers.¹⁸ The dimerization, however, is drastically reduced with bulkier titanocenes.^{18a} Hydrochloride additives such as coll-HCl (coll = 2,4,6-collidine) or $\text{Et}_3\text{N}\cdot\text{HCl}$ lead instead to the formation of a coordination complex of $[\text{Cp}_2\text{TiCl}]$ and the hydrochloride.^{8l,19} Due to this complexity, one of the major challenges was to elucidate the actual nature of the intermediates of the acyloin-type cross-coupling. Thus, the following fundamental questions were raised: (1) Is the reaction a titanium(III)-catalyzed process? (2) Are cationic intermediates involved? (3) Which is the rate-determining step? (4) What is the nature of the C–C bond forming event, and are two titanium(III)-species involved? (5) What are the roles of the additives, especially the hydrochloride?

EPR SPECTROSCOPY

The investigation was started with EPR spectroscopy with the goal to confirm the presence of titanium(III) in the catalysis shown in eq 2. EPR is the method of choice to detect and investigate paramagnetic metal centers. Previously, bis-(cyclopentadienyl)-titanium(III) species such as $[\text{Cp}_2\text{TiCl}]$ and $[\text{Cp}_2\text{Ti}(\text{THF})]^+$ had been investigated by EPR spectroscopy, which facilitated the analysis.^{8h,17,20,21} Hence, continuous-

wave EPR spectra of three samples were recorded in both frozen (110 K) and liquid states (220 K): (a) a solution of Zn-reduced **2** and acetophenone in THF, (b) a solution of Zn-reduced **2** and benzyl cyanide in THF, and (c) the reaction mixture as shown in eq 2. For all the mixtures and at both temperatures, intense signals originating from titanium(III) species were observed. The isotropic hyperfine features from the coupling to ^{47}Ti and ^{49}Ti isotopes with $I = 5/2$ and $I = 7/2$, respectively, were well resolved in the spectra measured for liquid-state samples. Since most spectra revealed signals from multiple titanium(III) components, the tentative assignment of the signals was based on DFT-calculated EPR parameters.²²

Sample (a) recorded at 220 K showed the presence of two titanium(III)-species and the main features of the isotropic signals were satisfactorily reproduced considering two components with g_{iso} of 1.981 and 1.979 (see Figure S1, Supporting Information).²² In contrast, the signal of a frozen solution of sample (a) was dominated only by a single titanium(III) species with the g-tensor principal values $g_x = 1.958$, $g_y = 1.982$, and $g_z = 2.003$ resulting in $g_{\text{iso}} = 1.981$ (Figure 1). Based on the

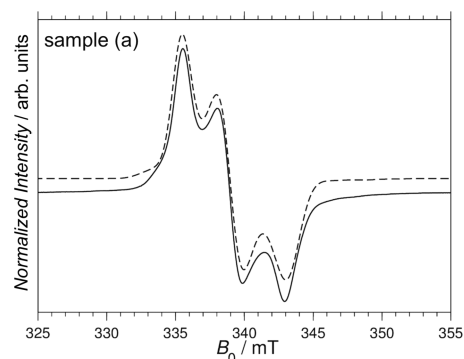


Figure 1. Continuous-wave EPR spectrum of Zn-reduced **2** in THF with added PhCOMe (sample (a)) at X-band (9.404 GHz) at 110 K (solid line). Simulated spectrum (dashed line). Experimental conditions: microwave power, 1.99 mW; magnetic-field modulation amplitude, 0.1 mT (100 kHz modulation frequency); time constant, 40.96 ms.

comparison of the parameters from the fit with literature data and the computed g-tensor principal values, this signal was assigned to $[(\text{EtCp})_2\text{TiCl}]$ (**3**).²² However, a cationic Ti^{III} -acetophenone complex $[(\text{EtCp})_2\text{Ti}(\text{PhCOMe})]^+$ (**4**) could also be a possible choice: considering the typical computational errors observed in previous calculations of EPR parameters,^{8h} $g_{\text{iso}} = 1.980$ as calculated for **4** (with $g_x = 1.950$, $g_y = 1.991$, $g_z = 2.001$) did not deviate strongly from the values obtained from the fit to the experimental data. The second species, with $g_{\text{iso}} = 1.979$ that was formed only at 220 K could not be assigned by comparison with calculated values for neutral or cationic titanium(III) complexes that could potentially be present under these conditions.²² We propose that the titanium(III) complex which we observed at 110 K ($g_{\text{iso}} = 1.981$) decomposed to this second species ($g_{\text{iso}} = 1.979$) during the time required for thawing and thermal equilibration of the sample. Importantly, a sample (a) prepared in the presence of an excess of Zn or Mn still showed the characteristic titanium(III) signal with unchanged intensity, which spoke against a further reduction to titanium(II) in the presence of a large excess of the reductant. Therefore, a potential Ti(II)-pathway was ruled out for this coupling.^{9a}

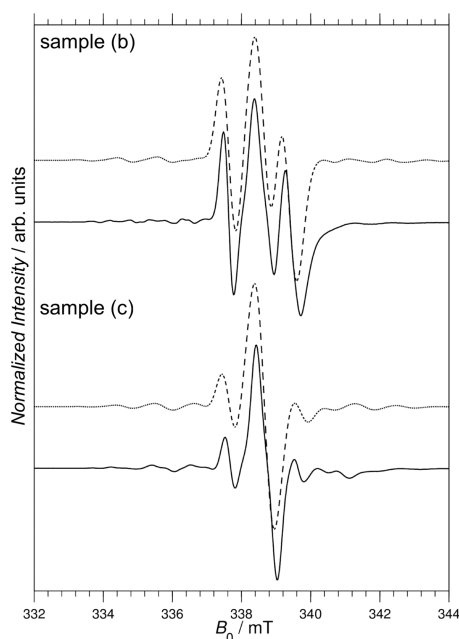


Figure 2. Continuous-wave EPR-spectra of Zn-reduced **2** in THF with added BnCN (sample (b)), and the reaction mixture of the catalytic reaction (sample (c)) at X-band (9.404 GHz) at 220 K (solid lines). Simulated spectra (dashed lines). Experimental conditions: microwave power, 1.99 mW; magnetic-field modulation amplitude, 0.1 mT (100 kHz modulation frequency); time constant, 40.96 ms.

The isotropic signal of sample (b) comprised three titanium(III)-components of nearly equal intensities with $g_{\text{iso}} = 1.979$ (identical to the unknown species observed for liquid-state sample (a)), $g_{\text{iso}} = 1.984$ (which could not be assigned), and $g_{\text{iso}} = 1.990$ (Figure 2). The last matched perfectly the g_{iso} value calculated for the cationic bis-acetonitrile complex $[(\text{EtCp})_2\text{Ti}(\text{BnCN})_2]^+$ (**5**).²² The relative intensities of the components changed between the spectra of liquid and frozen samples, indicating that a reaction set in upon thawing of the sample (see Figure S2, Supporting Information). The isotropic spectrum of sample (c) also comprised three signals (Figure 2) with nearly the same g_{iso} values as those found for sample (b) but with very different relative intensities. The most intense signal was centered at $g_{\text{iso}} = 1.990$. However, a reliable fit of the data was hampered by the presence of multiple Ti(III)-components in both samples (b) and (c).

Overall, the above-discussed data confirmed the presence of titanium(III) under our reaction conditions and indicated the formation of a cationic bis-benzylcyanide complex. The complexity of the mixtures, prevented further assignments.

ESI-MS INVESTIGATIONS

With the goal to further reveal the nature of the titanium(III) intermediates present under catalytic conditions, we then performed a series of electrospray MS (ESI-MS) experiments of the reaction mixtures in an online fashion. The actual reaction mixtures were directly transferred from a sealed flask to the electrospray source using a PEEK capillary.^{22,23} In this way, cationic species present in the solution could be detected and characterized. For the studies at hand, we employed the 4-methyl substituted acetophenone (p-TolCOMe) and benzyl cyanide to circumvent the overlap of certain mass peaks. An overall concentration of 0.1 M was applied and the catalyst loading was increased to 50 mol %. These “dilute conditions”

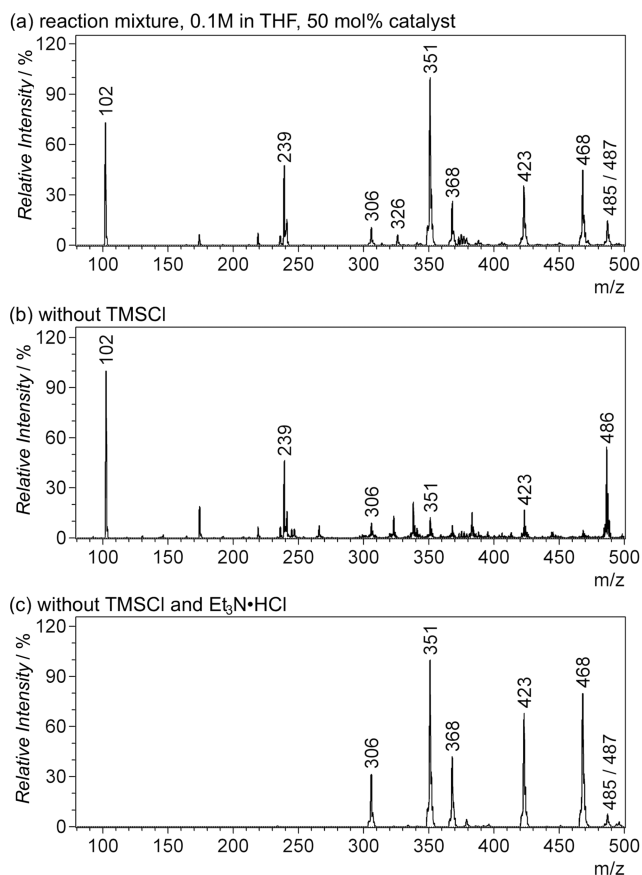
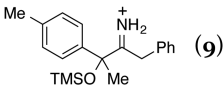
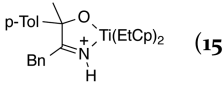


Figure 3. In situ ESI-MS spectra showing cationic intermediates.

Table 1. Assignment of MS Peaks

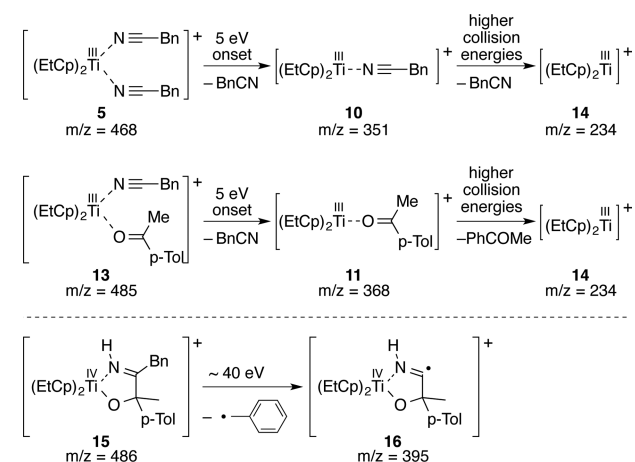
peak m/z	assigned species
102.0	$[\text{HNEt}_3]^+$ (6)
239.1	$[(\text{HNEt}_3)_2\text{Cl}]^+$ (7)
306.0	$[(\text{EtCp})_2\text{Ti}(\text{THF})]^+$ (8)
326.1	 (9)
351.0	$[(\text{EtCp})_2\text{Ti}(\text{BnCN})]^+$ (10)
368.0	$[(\text{EtCp})_2\text{Ti}(\text{p-TolCOMe})]^+$ (11)
423.1	$[(\text{EtCp})_2\text{Ti}(\text{BnCN})(\text{THF})]^+$ (12)
468.1	$[(\text{EtCp})_2\text{Ti}(\text{BnCN})_2]^+$ (5)
485.1	$[(\text{EtCp})_2\text{Ti}(\text{BnCN})(\text{p-TolCOMe})]^+$ (13)
486.1	 (15)
487.1	unidentified byproduct

facilitated the detection of cationic species, in particular substrate-titanocenium complexes, and led to stable, reproducible spectra.²²

The spectrum of the catalytic reaction mixture (Figure 3a) showed the presence of several titanocenium intermediates m/z 306.0, 351.0, 368.0, 423.1, 468.1, and 485.1 that were structurally assigned and characterized by collision-induced dissociation (CID) (Table 1).²⁴ Since fragmentation of these

complexes could be induced at relatively low collision energies (with an onset of ca. 5 eV lab frame) it is safe to assume the ligands were bound coordinatively to the titanium center as shown for the dinitrile complex **5** and the mixed complex **13** (Scheme 2). In all cases, $[(\text{EtCp})_2\text{Ti}]^+$ (**14**) remained as the

Scheme 2. CID Characterization of Selected Intermediates m/z 468, 485, and 486



ionic metal species after dissociation. In addition, ammonium species **6** and **7** emerging from $\text{Et}_3\text{N}\cdot\text{HCl}$ and importantly, the protonated, silylated imine (**9**) were identified. The species m/z 487.1 was a byproduct that only occurred under the dilute conditions and was not a product of the titanium(III)-catalyzed coupling.²²

Subsequently, an identical experiment was carried out in absence of TMSCl (Figure 3b). While the titanocenium complexes **5**, **8**, and **10–13** were all greatly diminished in their intensities, a new ion with m/z 486 was detected as the main species. It was assigned the protonated titanocene-product chelate **15**: fragmentation of m/z 486 sets in at a much higher collision energy of about 40 eV and proceeded via the loss of a benzyl radical (m/z 91), thus leading to radical cation **16** with m/z 395 (Scheme 2, bottom).

This pattern was further confirmed by employing acetophenones and benzyl cyanides with different aromatic substituents.²² Finally, the experiment was repeated in absence of TMSCl and $\text{Et}_3\text{N}\cdot\text{HCl}$. Here, only the previously identified titanocenium complexes of acetophenone, benzyl cyanide and THF were observed. The product chelate with m/z 486 was not detected.

The presence of neutral species in solution that were not detectable in the previous experiments was probed with a charge-tagged substrate (Figure 4) as demonstrated earlier by

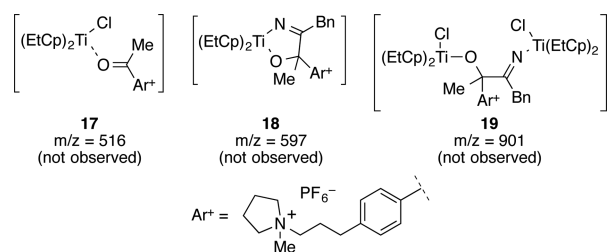


Figure 4. Chloride-containing titanocene intermediates could not be detected with a charge-tagged acetophenone.

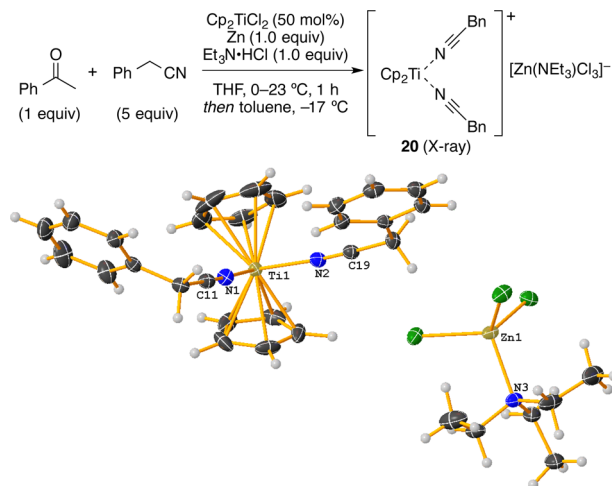
others and ourselves.²³ Performing the coupling with an *N*-methylpyrrolidinium tagged acetophenone, it was first ensured in an independent experiment that the desired hydroxyketone was formed. It turned out to be crucial to use the PF_6^- counterion in order to increase the substrate solubility and to prevent catalyst inhibition by a high local halide concentration.²² Despite extensive experimentation and various modifications of the charge-tag, none of the species **17–19** shown in Figure 4 could be detected. Only the benzyl cyanide and THF complexes **5**, **8**, **10**, **12**, the charge-tagged substrate itself, and the charged imine were detected in the online ESI-MS experiments.²²

These findings led us to the conclusion that cationic substrate-titanium(III) complexes were indeed present in solution and represented resting states of the catalyst. Furthermore, the formation of product chelate **15** occurred only with added $\text{Et}_3\text{N}\cdot\text{HCl}$. Since the corresponding charge-tagged neutral chelate was not detected in absence of $\text{Et}_3\text{N}\cdot\text{HCl}$, this confirmed that the preceding C–C bond formation required the presence of this additive. Subsequent detitanation-silylation of this intermediate was significantly faster since this chelate was not observed in the catalytic mixture.

ISOLATION OF A CATALYST RESTING STATE

Crystallization experiments were undertaken to isolate a potential resting state using authentic reaction mixtures with 50 mol % catalyst loading in absence of TMSCl . The titanium precursor was changed to $[\text{Cp}_2\text{TiCl}_2]$ to facilitate crystallization, which was carried out at -17°C from toluene under argon atmosphere (Scheme 3). The cationic bis-benzylcyanide

Scheme 3. X-ray Structure of Catalyst Resting State **20**^a

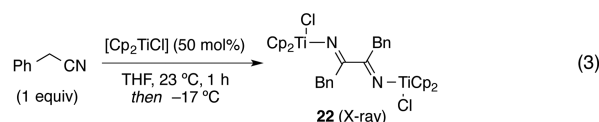


^aThermal ellipsoids drawn at 50% probability level. Disordered toluene molecules were omitted for clarity. Selected bond lengths (Å) and angles (deg): Ti(1)–N(1) 2.1709(15), Ti(1)–N(2) 2.1564(14), N(1)–C(11) 1.144(2), N(2)–C(19) 1.138(2), N(3)–Zn(1) 2.1053(14), N(1)–Ti(1)–N(2) 83.78(6), Cp(1)–Ti(1)–Cp(2) 135.725.

titanocene **20** was obtained, which was the unsubstituted version of the resting state identified in the ESI-MS experiments. Complex **20** was unambiguously characterized by X-ray analysis. The counterion was a triethylamine-stabilized trichlorozincate, which could have emerged from the abstraction of Cl^- from the titanium in the presence of benzyl

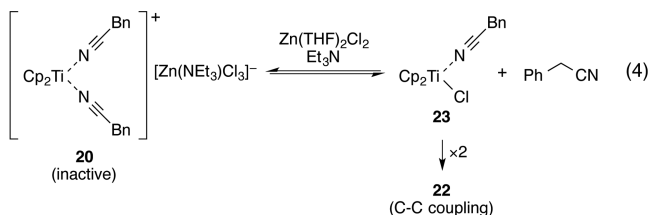
cyanide and ZnCl_2 .^{9c,17,18b,c} Along these lines, it was possible to isolate and characterize $[\text{HNEt}_3][\text{Zn}(\text{Et}_3\text{N})\text{Cl}_3]$ (**21**) via X-ray analysis, which apparently constituted a byproduct of our cross-coupling reactions, from a similar experiment with only two equivalents of benzyl cyanide.²²

The bis-benzylcyanide complex **20** was previously described in the literature as not isolable due to its tendency to dimerize rapidly.²⁵ In a third attempt to isolate **20**, $[\text{Cp}_2\text{TiCl}]$ in THF (generated by reduction with Zn followed by filtration) was treated with 2 equiv of benzyl cyanide at room temperature (eq 3). Indeed, crystallization at -17°C then afforded the



literature-known bis-titanated 1,2-diimine **22**.²⁵ At this lower nitrile-catalyst ratio of 2:1, solvation of the remaining chloride by the nitrile was apparently less favorable. Although **22** had been characterized previously, this X-ray analysis was of crucial importance to confirm its formation under conditions that were very similar to those of our reductive acyloin-type coupling. This led to the following conclusions:

(1) C–C bond formation did not occur from the cationic bis-benzyl cyanide complex, but from the neutral chloride complex $[\text{Cp}_2\text{Ti}(\text{BnCN})_2(\text{Cl})]$ (**23**), which was in equilibrium with **20** as earlier proposed by Rehbaum and Thiele (eq 4).²⁵ The requirement of a coordinating chloride was further supported by an earlier study of pinacol couplings in aqueous media,²⁶ and our ESI-MS experiments.



(2) Two titanium species were likely involved in the C–C bond forming process as indicated by the crystal structure of the dichlorotitanated diimine **22**.

It should be noted that this titanium(III)-promoted reaction was therefore completely different from recently published titanium(II)-mediated nitrile–nitrile couplings.²⁷

REACTION PROGRESS KINETIC ANALYSIS

To gain deeper insight into the reaction mechanism, a reaction progress kinetic analysis of the reaction in eq 2 was undertaken using in situ IR spectroscopy.²⁸ This allowed us to identify the rate-determining step, the rate equation and changes in the reaction order over the reaction course. The consumption of acetophenone ($\nu = 1689 \text{ cm}^{-1}$) as well as the buildup of the α -silyloxyimine product ($\nu = 1645 \text{ cm}^{-1}$) could be followed precisely.²² The former was found suitable for the monitoring of reaction kinetics after calibration. Then, the determination of the order in catalyst, acetophenone, benzyl cyanide, hydrochloride, and TMS chloride was carried out, all of which could potentially contribute to the rate (eq 5).

$$\text{rate} \propto [\mathbf{2}]^a [\text{PhCOMe}]^b [\text{BnCN}]^c [\text{Et}_3\text{N}\cdot\text{HCl}]^d [\text{TMSCl}]^e \quad (5)$$

We monitored reactions with varying amounts of TMSCl (2.0, 1.5, and 1.1 equiv) (Figure 5a), and an almost identical curve

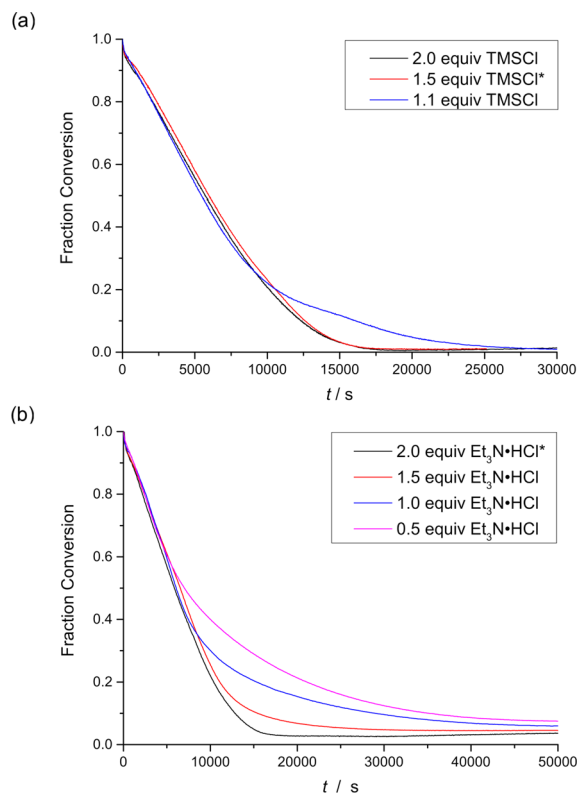


Figure 5. Plots of fraction conversion of $[\text{PhCOMe}]$ vs time. (a) Varying amounts of TMSCl. (b) Varying amounts of $\text{Et}_3\text{N}\cdot\text{HCl}$. The asterisk (*) marks the standard reaction conditions from eq 2.

was observed for the reactions up to $\sim 80\%$ conversion, which confirmed a zeroth order dependence in TMSCl as our MS experiments had suggested. A reaction run with only 1.1 equiv became slower at this point, indicating a change in the rate-determining step at low TMSCl amounts. A similar scenario was observed for reactions run with varying amounts of $\text{Et}_3\text{N}\cdot\text{HCl}$. Here, it was important to note that 2.0 equiv of hydrochloride additive were required to maintain a high reaction rate until full completion was achieved (Figure 5b). Thus, the reaction was zeroth order in TMSCl as well as $\text{Et}_3\text{N}\cdot\text{HCl}$, which simplified eq 5 to eq 6.

$$\text{rate} \propto [\mathbf{2}]^a [\text{PhCOMe}]^b [\text{BnCN}]^c \quad (6)$$

With the assumption that $[\mathbf{2}]^a$ remained constant, the determination of the reaction order in acetophenone was then possible by plotting $\text{rate} \times [\text{PhCOMe}]^{-b}$ vs $[\text{BnCN}]$ at different excess of $[\text{BnCN}]$ over $[\text{PhCOMe}]$ (varied equivalents of PhCOMe) and altering b until an overlap of the curves was achieved. This way, the order of the reaction in acetophenone was determined to be $b = 0.6$.²² In a similar fashion, a plot of $\text{rate} \times [\text{BnCN}]^{-c}$ vs $[\text{PhCOMe}]$ using the same data set, revealed an order in BnCN of $c \approx -3$.²² The plot in Figure 6 of $\text{rate} \times [\text{BnCN}]^3$ vs $[\text{PhCOMe}]^{0.6}$ showing overlaying curves in a straight line confirmed these results.

A possible interpretation of these unusual findings was a double Michaelis–Menten situation:^{28e} The product forming species A and B emerged each from kinetically close equilibria with the bis-benzyl cyanide resting state as shown in Scheme 4.

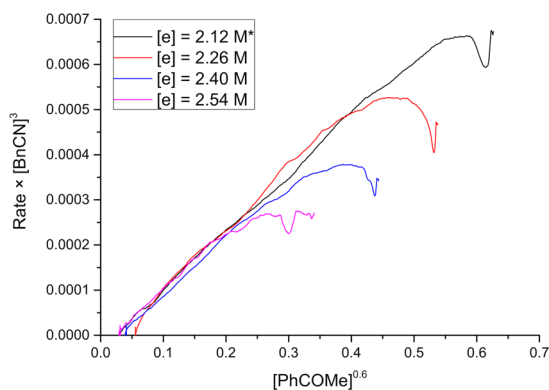
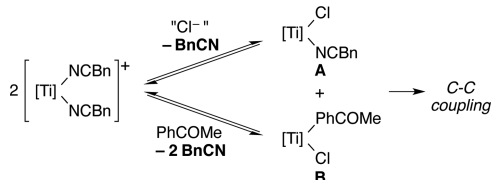


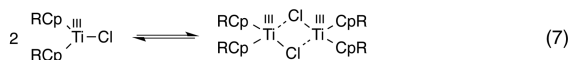
Figure 6. Graphical rate equation verifying a 0.6th order in PhCOMe and -3 rd order in BnCN.

Scheme 4. Rationale for the Observed Orders



However, regarding the complex situation and the likely involvement of other cationic species, a full elucidation of the situation would require a detailed analysis that was beyond the scope of this work.

Then, the reaction was examined at different catalyst loadings. A plot of reaction rate vs [PhCOMe] revealed that the order of the reaction changed dramatically depending on the catalyst amount and the reaction progress (Figure 7a). For higher catalyst loadings an increasingly dominant initiation period was observed and the maximum reaction rate was achieved with 20 mol % of **2** at $\sim 50\%$ conversion. We attributed this initiation period to an increased formation of (catalytically inactive) titanocene(III) dimers at such high catalyst concentrations (eq 7).²² Previously, it was shown that



substituted titanocene(III)-chlorides have a significantly lower tendency to dimerize than $[\text{Cp}_2\text{TiCl}]$.^{18a} Consequently, a standard reaction run with 10 mol % $[\text{Cp}_2\text{TiCl}_2]$ as catalyst, showed an increased initiation period.²² The reaction with only 5 mol % of **2**, on the other hand, did not exhibit an initiation time and followed a first overall reaction order over the whole reaction course, indicating a change in the rate-determining step at low catalyst loadings. From the plots of $\text{rate} \times [\mathbf{2}]^{-a}$ vs [PhCOMe], a reasonable overlap of the curves was achieved for the second half of the reaction for $a = 1.6$ (Figure 7b). This was in agreement with a second order reaction and the above-mentioned off-cycle formation of dimers, reducing the observed order in catalyst from 2 to 1.6.

From these results, the following conclusions were drawn:

(1) Protonation and silylation of the product were not rate-determining. However, 2 equiv of $\text{Et}_3\text{N}\cdot\text{HCl}$ was required to achieve full conversion. The first was attributed to the protonation of the Ti–N bond of the product chelate. The second equivalent was likely required due to the formation of

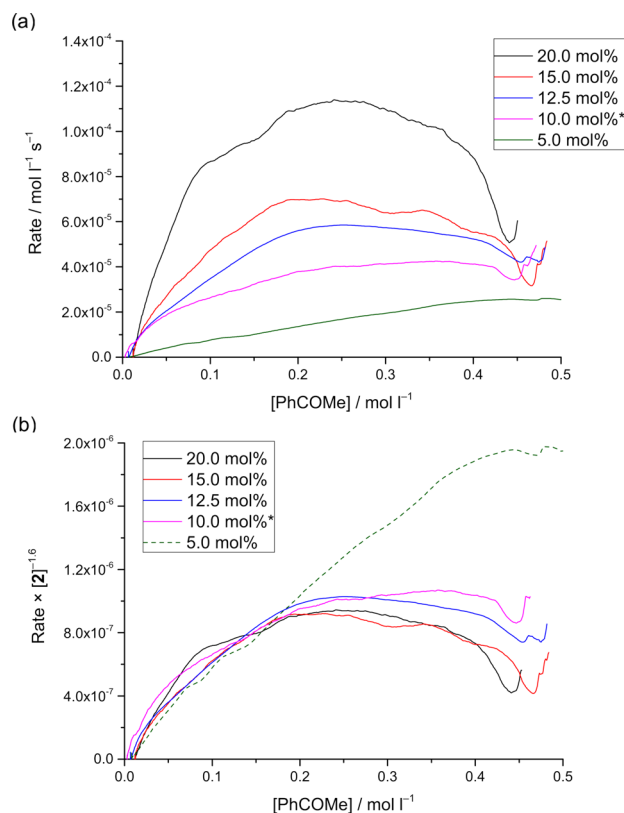


Figure 7. Determination of reaction order in catalyst. Plots of (a) rate vs [PhCOMe] and (b) $\text{rate} \times [\mathbf{2}]^{-1.6}$ vs [PhCOMe] of reactions at varying catalyst loading.

$[\text{HNEt}_3][\text{Zn}(\text{Et}_3\text{N})\text{Cl}_3]$ from the reaction of $[\text{Zn}(\text{THF})_2\text{Cl}_2]$ with $\text{Et}_3\text{N}\cdot\text{HCl}$ and Et_3N .

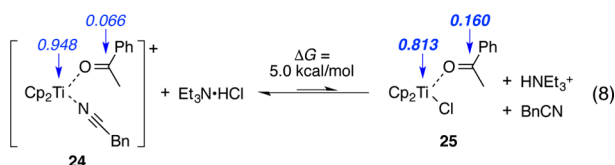
(2) The titanium(III)-catalyzed acyloin-type coupling was a complex case of catalyst saturation kinetics with a rate-limiting bimolecular C–C formation from two different substrate-catalyst complexes. Acetophenone and benzyl cyanide competed for the coordination to the titanium center in a pre-equilibrium situation. The negative order in BnCN was further in agreement with a nonproductive (off-cycle) resting state such as **5**.

(3) The observed 1.6th order in catalyst and the initiation time were the results of a bimolecular reaction and a nonproductive (off-cycle) dimer formation of the catalyst, which increased with the catalyst loading.

■ HAMMETT ANALYSIS AND ACTIVATION PARAMETERS

To further support our conclusions, an investigation of the electronic influence of the substrate on the catalysis and the determination of the activation enthalpy and entropy was undertaken. A Hammett-analysis showed a dependence of the reaction rate on the electronic properties of the acetophenone.²² Interestingly, a value of $\rho = 0.81$ was obtained, which showed that electron-poor acetophenones reacted significantly faster than electron-rich ones. This was in agreement with our conclusion that C–C bond formation proceeds via a chloride-coordinated acetophenone complex: chloride coordination to titanium-acetophenone complexes with more electron-withdrawing acetophenone ligands would be facilitated. In addition, electron-poor ketones would be reduced more easily and should therefore be better substrates in general. The preference

for C–C coupling from the chloride complex was supported by a DFT-calculation of the conversion of $[\text{Cp}_2\text{Ti}(\text{BnCN})(\text{PhCOMe})]^+$ (**24**) into $[\text{Cp}_2\text{Ti}(\text{PhCOMe})(\text{Cl})]$ (**25**) by a chloride transfer from $\text{Et}_3\text{N}\cdot\text{HCl}$ on the PW6B95²⁹-D3³⁰-COSMO³¹/def2-QZVP³²//TPSS³³-D3-COSMO/def2-TZVP³²-level using the TURBOMOLE V6.5 package.^{22,34} It was found that the chloride complex had a significantly increased spin density at the carbonyl carbon, which would lead to an increased reactivity toward a C–C bond forming radical reaction at this carbon (eq 8).²² This was in agreement with the



expected increase of the reduction potential of the titanocene upon chloride coordination and thus a higher performance of the catalyst. The influence of the redox potential of titanocenes on the performance in redox reactions was discussed previously.^{8b,9c,19,35} The chloride transfer, however, was found to be endergonic and thus, the equilibrium was on the side of the thermodynamically favored cationic species. This explained the requirement of a high chloride concentration to induce C–C bond formation and also why the chloride complex remained elusive in our ESI-MS experiments. The electronic influence of the nitrile was briefly examined as well, but side-reactions were observed with varying benzonitriles and no appropriate data could be obtained. For para-substituted benzyl cyanides, no influence was observed.²² The activation parameters for the rate-limiting step were determined from an Eyring-plot with data from IR-monitored experiments at different temperatures.²² A positive, but low activation enthalpy and a considerable negative activation entropy were obtained (Table 2). This was in agreement with a highly ordered

Table 2. Experimental Activation Parameters

parameter	value
ΔH^\ddagger	10.2 kcal mol ⁻¹
ΔS^\ddagger	-45.5 cal mol ⁻¹ K ⁻¹
$\Delta G^\ddagger_{298.15\text{K}}$	23.8 kcal mol ⁻¹
k	2.4×10^{-5} s ⁻¹

transition state suffering from steric repulsion as well as a bimolecular reaction in form of a radical combination of two titanium(III)-complexes. From these values, $\Delta G^\ddagger_{298.15\text{K}} = 23.8$ kcal mol⁻¹ and a rate constant of $k = 2.4 \times 10^{-5}$ s⁻¹ were calculated that matched our kinetic data at that temperature. Interestingly, this reaction seemed to be significantly slower than related titanium(III)-catalyzed epoxide opening reactions.^{7e,18a}

■ THE ASYMMETRIC CYCLIZATION REACTION

The asymmetric cyclization with enantiopure *ansa*-titanocene catalyst **1** (eq 1) was examined as well in order to fully understand the role of the hydrochloride additive and to confirm that a second order C–C formation was also present in the intramolecular case.

First, ESI-MS analyses of the reaction mixture were carried out and the results were identical to the intermolecular reaction: in absence of $\text{Et}_3\text{N}\cdot\text{HCl}$ and TMSCl , a cationic

titanium(III)-substrate chelate was detected as main species. Upon addition of $\text{Et}_3\text{N}\cdot\text{HCl}$, a comparably stable cationic chelate of the protonated product with a titanium(IV)-center was observed as sole species.²²

Then, the influence of the amount of the hydrochloride additive on the yield and the enantioselectivity of the cyclization reaction was investigated (Figure 8). Although

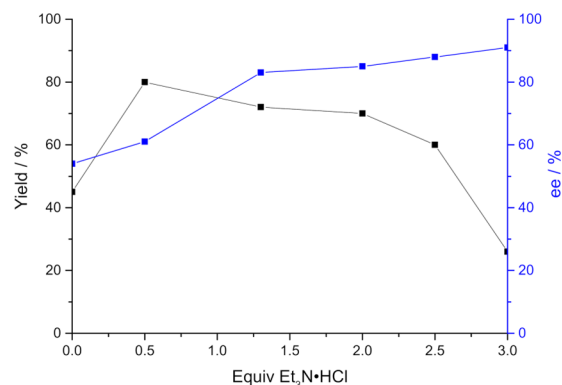
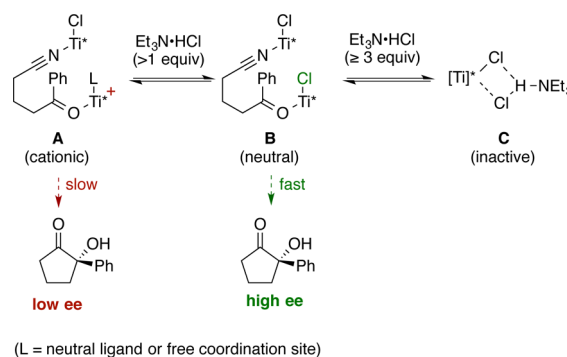


Figure 8. Influence of $\text{Et}_3\text{N}\cdot\text{HCl}$ amount on yield and enantiomeric excess of the cyclization in eq 1.

product formation was already observed in absence of the hydrochloride, the addition of 0.5 equiv $\text{Et}_3\text{N}\cdot\text{HCl}$ increased the reaction yield significantly. Higher amounts diminished the yield again and the addition of 3.0 equiv $\text{Et}_3\text{N}\cdot\text{HCl}$ almost inhibited the reaction. Importantly, the enantiomeric excess increased in an almost linear fashion upon further addition of $\text{Et}_3\text{N}\cdot\text{HCl}$ (up to 91% ee at 3.0 equiv $\text{Et}_3\text{N}\cdot\text{HCl}$). Thus, chloride coordination directly affected the enantioselectivity-determining C–C bond formation.

The scenario shown in Scheme 5 provided a plausible rationale for this observed additive effect. Two equivalents of

Scheme 5. Proposed Scenario for the Observed Dependence of Yield and Enantioselectivity on the Hydrochloride Amount



titanium catalyst coordinated the substrate and two pathways to the product existed. At low chloride concentrations, the first path was followed, in which the product was formed from a bis-titanium complex **A** containing one cationic titanium species. Because of the reduced reactivity toward a radical combination (see above), the product formation was slow in this case and a low enantioselectivity was obtained. At higher chloride concentrations (>0.5 equiv $\text{Et}_3\text{N}\cdot\text{HCl}$), a second path became available that proceeded via a neutral dichloro-bis-titanium complex **B**. The C–C bond formation was faster due to a

higher spin-density at the carbonyl carbon and the increased reduction potential of the catalyst. The additionally coordinated chloride led to a more rigid transition state, which was expressed in a high enantioselectivity. At too high chloride concentrations (>3 equiv), however, a titanocene(III)-hydrochloride complex C was formed. As noted in the introduction, hydrochloride adducts were known to stabilize the catalyst but also to represent inactive catalyst species.^{81,19} Due to charge-repulsion, a C–C bond formation involving two cationic complexes was ruled out.

Finally, the asymmetric cyclization exhibited a case of asymmetric amplification, which was concluded from a positive nonlinear effect that was determined from reactions with varying enantiopurity of the catalyst (Figure 9).³⁶ This

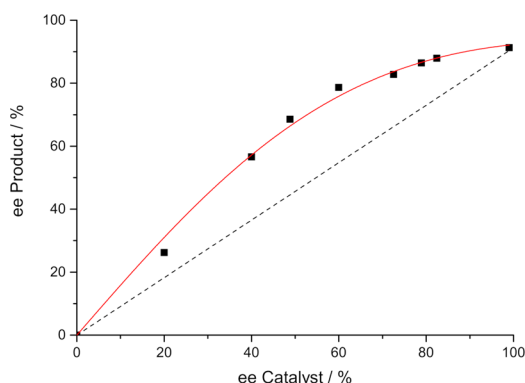


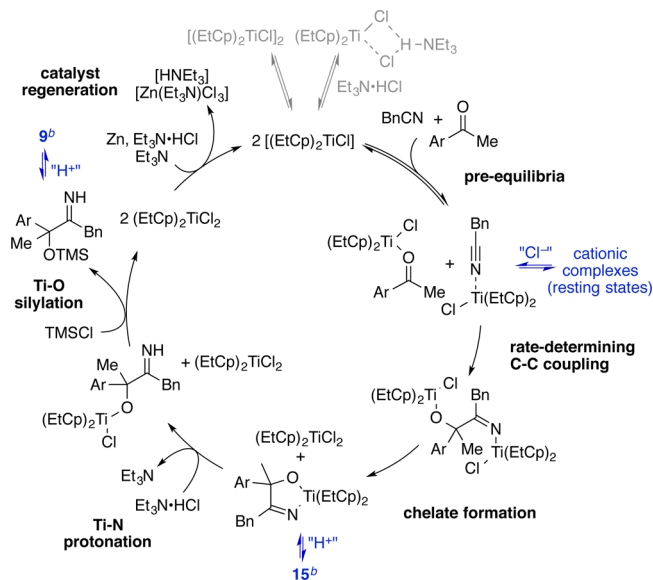
Figure 9. Nonlinear effect observed in the asymmetric cyclization of eq 1. The data was fitted using the ML₂ model (red line).

unambiguously confirmed the second order catalyst dependence of the C–C bond forming event in the asymmetric cyclization reaction. Using the ML₂ model for the coordination of two equivalents of catalyst to one substrate (here: M = substrate, L = catalyst), a fit was obtained from which the values $K = 3.74$ and $g = 0.13$ were extracted.²² The value of K being close to 4 indicated an almost statistical distribution for the coordination of the catalyst enantiomers to the substrate [2(*R,R*):(*R,R*)/(*S,S*):2(*S,S*) = 1:2:1]. The substrate complexed by two identical (homochiral) catalyst enantiomers reacted about $1/g = 7.7$ times faster than the substrate coordinated by two catalyst enantiomers of opposite absolute configuration.

CONCLUSIONS

The titanium(III)-catalyzed acyloin-type cross-coupling of ketones and nitriles as shown in eqs 1 and 2 was investigated by a combination of methods including EPR, ESI-MS, kinetic studies, X-ray analysis, and DFT calculations. Through this combined approach, the C–C bond formation was identified to be the rate-determining key step and it was revealed that it proceeds via a radical combination involving two titanium(III) catalyst species (Scheme 6). This radical combination led to the observed catalyst control of the selectivity and circumvented free radical intermediates. Cationic complexes of the ketone and nitrile reagents represented catalyst resting states, but their role was intriguing: although such cationic species were the only observable titanium complexes in solution, they were not productive. Instead, product formation occurred from neutral chloride complexes, which explained the positive influence of Et₃N-HCl on yield and enantioselectivity. Ketone and nitrile competed for coordination to the titanium(III), and thus, a

Scheme 6. Catalytic Cycle Summarizing the Results^a



^aSpecies detected by ESI-MS were highlighted in blue, and inhibiting pathways were drawn in gray. ^bAr = *p*-tolyl.

complex equilibrium situation existed prior to the C–C formation.

The results are fundamental for the understanding of related titanium(III)-catalyzed C–C couplings and the design of future titanium catalyzes will benefit from this study. The counterion could provide a feasible platform for the fine-tuning of the catalyst properties that is complementary to the often executed optimization of the titanocene backbone.^{8a,b,9c,19,35} Furthermore, bimetallic catalysts containing appropriately linked titanocenes could lead to a superior performance in reductive C–C couplings such as the title reaction.

In a broader perspective, our results will be valuable for the development of other catalyst-controlled radical reactions. Furthermore, a similar bimolecular radical combination mechanism could be present in a number of cases that exhibited superior catalyst control of the chemo-, regio-, and stereochemistry. This includes reductive couplings catalyzed by other metals such as V, Cr, Fe, Co, Ni, Zr, Ru, In, Sn, Pb, Ce, Yb, and importantly Sm that take place under related conditions.⁵ In addition, a number of reductive couplings that were proposed to be Mⁿ/Mⁿ⁺²-catalyzed processes could in fact involve open-shell species as was previously suggested for certain cobalt catalyzed reactions.³⁷ The combined approach presented here could provide important insight in these cases and find application in the mechanistic investigation of other complex reactions that are heterogeneous, require multiple additives, or involve radical intermediates.

ASSOCIATED CONTENT

Supporting Information

The Supporting Information is available free of charge on the ACS Publications website at DOI: 10.1021/jacs.5b09223.

Materials and methods for EPR, in situ ESI-MS, in situ IR experiments, and computational details; additional experimental results and DFT calculations; NMR spectra of new compounds and HPLC reports (PDF)
X-ray crystallographic data for 20-toluene (CIF)
X-ray crystallographic data for 21 (CIF)

X-ray crystallographic data for 22 (CIF)

AUTHOR INFORMATION

Corresponding Author

*jan.streuff@ocbc.uni-freiburg.de

Notes

The authors declare no competing financial interest.

ACKNOWLEDGMENTS

We gratefully acknowledge generous financial support by the Fonds der Chemischen Industrie (Dozentenpreis and Liebig-Fellowship to JS) and the Deutsche Forschungsgemeinschaft, DFG (STR 1150/3-1, STR 1150/6-1, STR 1150/7-1). We furthermore thank Prof. Stefan Weber for his support and access to EPR equipment.

REFERENCES

- (1) *Metal-Catalyzed Cross-Coupling Reactions*; de Meijere, A., Diederich, F., Eds.; Wiley-VCH: Weinheim, 2004.
- (2) (a) Jeganmohan, M.; Cheng, C.-H. *Chem. - Eur. J.* **2008**, *14*, 10876–10886. (b) *Metal-Catalyzed Reductive C-C Bond Formation*; Krische, M. J., Ed.; Springer: Berlin, 2007. (c) Montgomery, J. *Angew. Chem., Int. Ed.* **2004**, *43*, 3890–3908.
- (3) (a) Seebach, D. *Angew. Chem., Int. Ed. Engl.* **1979**, *18*, 239–258. (b) Fittig, R. *Justus Liebigs Ann. Chem.* **1859**, *110*, 23–45.
- (4) Catalytic umpolung reactions and other cross-electrophile couplings are a highly topical research area: (a) Ackerman, L. K. G.; Lovell, M. M.; Weix, D. J. *Nature* **2015**, *524*, 454–457. (b) Wu, Y.; Hu, L.; Li, Z.; Deng, L. *Nature* **2015**, *523*, 445–450. (c) Lo, J. C.; Gui, J.; Yabe, Y.; Pan, C.-M.; Baran, P. S. *Nature* **2014**, *516*, 343–348.
- (5) (a) Streuff, J. *Synthesis* **2013**, *45*, 281–307. (b) Hirao, T. *Top. Curr. Chem.* **2007**, *279*, 53–75. (c) Gansäuer, A.; Bluhm, H. *Chem. Rev.* **2000**, *100*, 2771–2788. See also: (d) Knappke, C. E. I.; Grupe, S.; Gärtner, D.; Corpet, M.; Gosmini, C.; von Wangelin, A. J. *Chem. - Eur. J.* **2014**, *20*, 6828–6842. (e) Everson, D. A.; Weix, D. J. *J. Org. Chem.* **2014**, *79*, 4793–4798.
- (6) Streuff, J. *Chem. Rec.* **2014**, *14*, 1100–1113.
- (7) For selected reviews on low-valent titanium chemistry, see: (a) Morcillo, S. P.; Miguel, D.; Campaña, A. G.; Álvarez de Cienfuegos, L.; Justicia, J.; Cuerva, J. M. *Org. Chem. Front.* **2014**, *1*, 15–33. (b) Rossi, B.; Prosperini, S.; Pastori, N.; Clerici, A.; Punta, C. *Molecules* **2012**, *17*, 14700–14732. (c) Gansäuer, A.; Shi, L.; Otte, M.; Huth, I.; Rosales, A.; Sancho-Sanz, I.; Padial, N. M.; Oltra, J. E. *Top. Curr. Chem.* **2011**, *320*, 93–120. (d) Gansäuer, A.; Fan, C.-A.; Keller, F.; Karbaum, P. *Chem. - Eur. J.* **2007**, *13*, 8084–8090. (e) Gansäuer, A.; Justicia, J.; Fan, C.-A.; Worgull, D.; Piestert, F. *Top. Curr. Chem.* **2007**, *279*, 25–52. (f) Fürstner, A.; Bogdanović, B. *Angew. Chem., Int. Ed. Engl.* **1996**, *35*, 2442–2469.
- (8) For selected recent works on Ti^{III}-catalysis, see: (a) Gansäuer, A.; Hildebrandt, S.; Michelmann, A.; Dahmen, T.; von Laufenberg, D.; Kube, C.; Fianu, G. D.; Flowers, R. A., II *Angew. Chem., Int. Ed.* **2015**, *54*, 7003–7006. (b) Gansäuer, A.; von Laufenberg, D.; Kube, C.; Dahmen, T.; Michelmann, A.; Behlendorf, M.; Sure, R.; Seddiqzai, M.; Grimme, S.; Sadasivam, D. V.; Fianu, G. D.; Flowers, R. A., II *Chem. - Eur. J.* **2015**, *21*, 280–289. (c) Zhao, Y.; Weix, D. J. *J. Am. Chem. Soc.* **2015**, *137*, 3237–3240. (d) Márquez, I. R.; Miguel, D.; Millán, A.; Marcos, M. L.; de Cienfuegos, L. A.; Campaña, A. G.; Cuerva, J. M. *J. Org. Chem.* **2014**, *79*, 1529–1541. (e) Morcillo, S. P.; Martínez-Peragón, Á.; Jakoby, V.; Mota, A. J.; Kube, C.; Justicia, J.; Cuerva, J. M.; Gansäuer, A. *Chem. Commun.* **2014**, *50*, 2211–2213. (f) Muñoz-Bascón, J.; Hernández-Cervantes, C.; Padial, N. M.; Álvarez-Corral, M.; Rosales, A.; Rodríguez-García, I.; Oltra, J. E. *Chem. - Eur. J.* **2014**, *20*, 801–810. (g) Campos, C. A.; Gianino, J. B.; Ashfeld, B. L. *Org. Lett.* **2013**, *15*, 2656–2659. (h) Cangönül, A.; Behlendorf, M.; Gansäuer, A.; van Gastel, M. *Inorg. Chem.* **2013**, *52*, 11859–11866. (i) Gianino, J. B.; Ashfeld, B. L. *J. Am. Chem. Soc.* **2012**, *134*, 18217–18220. (j) Muñoz-Bascón, J.; Sancho-Sanz, I.; Álvarez-Manzaneda, E.; Rosales, A.; Oltra, J. E. *Chem. - Eur. J.* **2012**, *18*, 14479–14486. (k) Jiménez, T.; Morcillo, S. P.; Martín-Lasanta, A.; Collado-Sanz, D.; Cárdenas, D. J.; Gansäuer, A.; Justicia, J.; Cuerva, J. M. *Chem. - Eur. J.* **2012**, *18*, 12825–12833. (l) Gansäuer, A.; Behlendorf, M.; von Laufenberg, D.; Fleckhaus, A.; Kube, C.; Sadasivam, D. V.; Flowers, R. A., II *Angew. Chem., Int. Ed.* **2012**, *51*, 4739–4742. (m) Gansäuer, A.; Klatte, M.; Brändle, G. M.; Friedrich, J. *Angew. Chem., Int. Ed.* **2012**, *51*, 8891–8894. (n) Gansäuer, A.; Otte, M.; Shi, L. *J. Am. Chem. Soc.* **2011**, *133*, 416–417. (o) Kosal, A. D.; Ashfeld, B. L. *Org. Lett.* **2010**, *12*, 44–47.
- (9) (a) Rosales, A.; Muñoz-Bascón, J.; Roldan-Molina, E.; Castañeda, M. A.; Padial, N. M.; Gansäuer, A.; Rodríguez-García, I.; Oltra, J. E. *J. Org. Chem.* **2014**, *79*, 7672–7676. (b) Paradas, M.; Campaña, A. G.; Estévez, R. E.; Álvarez de Cienfuegos, L.; Jiménez, T.; Robles, R.; Cuerva, J. M.; Oltra, J. E. *J. Org. Chem.* **2009**, *74*, 3616–3619. (c) Enemærke, R. J.; Larsen, J.; Hjøllund, G. H.; Skrydstrup, T.; Daasbjerg, K. *Organometallics* **2005**, *24*, 1252–1262. (d) Yamamoto, Y.; Hattori, R.; Miwa, T.; Nakagai, Y.-i.; Kubota, T.; Yamamoto, C.; Okamoto, Y.; Itoh, K. *J. Org. Chem.* **2001**, *66*, 3865–3870. (e) Dunlap, M. S.; Nicholas, K. M. *J. Organomet. Chem.* **2001**, *630*, 125–131. (f) Gansäuer, A.; Moschioni, M.; Bauer, D. *Eur. J. Org. Chem.* **1998**, *1998*, 1923–1927. (g) Wirth, T. *Angew. Chem., Int. Ed. Engl.* **1996**, *35*, 61–63.
- (10) (a) Frey, G.; Hausmann, J. N.; Streuff, J. *Chem. - Eur. J.* **2015**, *21*, 5693–5696. (b) Bichovski, P.; Haas, T. M.; Kratzert, D.; Streuff, J. *Chem. - Eur. J.* **2015**, *21*, 2339–2342. (c) Feurer, M.; Frey, G.; Luu, H.-T.; Kratzert, D.; Streuff, J. *Chem. Commun.* **2014**, *50*, 5370–5372. (d) Frey, G.; Luu, H.-T.; Bichovski, P.; Feurer, M.; Streuff, J. *Angew. Chem., Int. Ed.* **2013**, *52*, 7131–7134. (e) Streuff, J.; Feurer, M.; Bichovski, P.; Frey, G.; Gellrich, U. *Angew. Chem., Int. Ed.* **2012**, *51*, 8661–8664. (f) Streuff, J. *Chem. - Eur. J.* **2011**, *17*, 5507–5510.
- (11) (a) Estévez, R. E.; Oller-López, J. L.; Robles, R.; Melgarejo, C. R.; Gansäuer, A.; Cuerva, J. M.; Oltra, J. E. *Org. Lett.* **2006**, *8*, 5433–5436. (b) Groth, U.; Jung, M.; Vogel, T. *Chem. - Eur. J.* **2005**, *11*, 3127–3135. (c) Jung, M.; Groth, U. *Synlett* **2002**, 2015–2018. (d) Boeckman, R. K., Jr.; Hudack, R. A., Jr. *J. Org. Chem.* **1998**, *63*, 3524–3525. (e) Corey, E. J.; Zheng, G. Z. *Tetrahedron Lett.* **1997**, *38*, 2045–2048.
- (12) See also: Zhou, L.; Hirao, T. *Tetrahedron* **2001**, *57*, 6927–6933.
- (13) It should be noted that the unpaired electron is in part located at the titanium and at the carbonyl carbon (see also eq 8). This can be illustrated by the following two mesomeric forms:
- $$\left[\text{Cl}-\overset{\text{Ti}^{\text{III}}}{\text{O}}-\overset{\text{O}}{\text{C}}-\text{R} \longleftrightarrow \text{Cl}-\overset{\text{Ti}^{\text{IV}}}{\text{O}}-\overset{\cdot}{\text{C}}-\text{R} \right]$$
- (14) (a) Fernández-Mateos, A.; Encinas Madrazo, S.; Herrero Teijón, P.; Rubio González, R. *J. Org. Chem.* **2009**, *74*, 3913–3918. (b) Fernández-Mateos, A.; Herrero Teijón, P.; Mateos Burón, L.; Rabanedo Clemente, R.; Rubio González, R. *J. Org. Chem.* **2007**, *72*, 9973–9982. (c) Yamamoto, Y.; Matsumi, D.; Hattori, R.; Itoh, K. *J. Org. Chem.* **1999**, *64*, 3224–3229. (d) Yamamoto, Y.; Matsumi, D.; Itoh, K. *Chem. Commun.* **1998**, 875–876.
- (15) Markovich, G.; Perera, L.; Berkowitz, M. L.; Cheshnovsky, O. *J. Chem. Phys.* **1996**, *105*, 2675–2685.
- (16) (a) Gansäuer, A.; Behlendorf, M.; Cangönül, A.; Kube, C.; Cuerva, J. M.; Friedrich, J.; van Gastel, M. *Angew. Chem., Int. Ed.* **2012**, *51*, 3266–3270. (b) Burgmayer, S. J. N. *J. Chem. Educ.* **1998**, *75*, 460. (c) Billinger, P. N.; Claire, P. P. K.; Collins, H.; Willey, G. R. *Inorg. Chim. Acta* **1988**, *149*, 63–67. (d) Coutts, R. S. P.; Kautzner, B.; Wailes, P. C. *Aust. J. Chem.* **1969**, *22*, 1137–1141.
- (17) Seewald, P. A.; White, G. S.; Stephan, D. W. *Can. J. Chem.* **1988**, *66*, 1147–1152.
- (18) (a) Daasbjerg, K.; Svith, H.; Grimme, S.; Gerenkamp, M.; Mück-Lichtenfeld, C.; Gansäuer, A.; Barchuk, A.; Keller, F. *Angew. Chem., Int. Ed.* **2006**, *45*, 2041–2044. (b) Enemærke, R. J.; Larsen, J.; Skrydstrup, T.; Daasbjerg, K. *Organometallics* **2004**, *23*, 1866–1874. (c) Enemærke, R. J.; Larsen, J.; Skrydstrup, T.; Daasbjerg, K. *J. Am. Chem. Soc.* **2004**, *126*, 7853–7864. (d) Coutts, R. S. P.; Wailes, P. C.;

Martin, R. L. *J. Organomet. Chem.* **1973**, *47*, 375–382. (e) Vonk, C. G. *J. Cryst. Mol. Struct.* **1973**, *3*, 201–207. (f) Salzmann, J.-J. *Helv. Chim. Acta* **1968**, *51*, 526–529.

(19) Gansäuer, A.; Kube, C.; Daasbjerg, K.; Sure, R.; Grimme, S.; Fianu, G. D.; Sadasivam, D. V.; Flowers, R. A., II *J. Am. Chem. Soc.* **2014**, *136*, 1663–1671.

(20) Samuel, E.; Vedel, J. *Organometallics* **1989**, *8*, 237–241.

(21) See also: (a) Kessler, M.; Schüler, S.; Hollmann, D.; Klahn, M.; Beweries, T.; Spannenberg, A.; Brückner, A.; Rosenthal, U. *Angew. Chem., Int. Ed.* **2012**, *51*, 6272–6275. (b) Kessler, M.; Hansen, S.; Hollmann, D.; Klahn, M.; Beweries, T.; Spannenberg, A.; Brückner, A.; Rosenthal, U. *Eur. J. Inorg. Chem.* **2011**, *2011*, 627–631.

(22) See the [Supporting Information](#).

(23) (a) Gellrich, U.; Meißner, A.; Steffani, A.; Kähny, M.; Drexler, H.-J.; Heller, D.; Plattner, D. A.; Breit, B. *J. Am. Chem. Soc.* **2014**, *136*, 1097–1104. (b) Vikse, K. L.; Ahmadi, Z.; Luo, J.; van der Wal, N.; Daze, K.; Taylor, N.; McIndoe, J. S. *Int. J. Mass Spectrom.* **2012**, *323*, 8–13. (c) Beierlein, C. H.; Breit, B.; Paz Schmidt, R. A.; Plattner, D. A. *Organometallics* **2010**, *29*, 2521–2532. (d) Chisholm, D. M.; McIndoe, J. S. *Dalton Trans.* **2008**, 3933–3945.

(24) These titanocenium complexes were also present in a 0.5 M reaction with 10 mol % catalyst; however, their intensity was drastically reduced. Instead, the protonated imine product, a titanocenium-Et₃N-HCl adduct and a product complex of (EtCp)₂TiCl₂ were the major peaks. See ref 22.

(25) (a) Rehbaum, F.; Thiele, K.-H.; Trojanov, S. I. *J. Organomet. Chem.* **1991**, *410*, 327–333. (b) De Boer, E. J. M.; Teuben, J. H. J. *Organomet. Chem.* **1978**, *153*, 53–57. (c) De Boer, E. J. M.; Teuben, J. H. J. *Organomet. Chem.* **1977**, *140*, 41–45.

(26) Barden, M. C.; Schwartz, J. *J. Am. Chem. Soc.* **1996**, *118*, 5484–5485.

(27) (a) Becker, L.; Arndt, P.; Spannenberg, A.; Jiao, H.; Rosenthal, U. *Angew. Chem., Int. Ed.* **2015**, *54*, 5523–5526. (b) Becker, L.; Arndt, P.; Jiao, H.; Spannenberg, A.; Rosenthal, U. *Angew. Chem., Int. Ed.* **2013**, *52*, 11396–11400.

(28) For excellent references on this topic, see: (a) Blackmond, D. G. *J. Am. Chem. Soc.* **2015**, *137*, 10852–10866. (b) Scott, M.; Sud, A.; Boess, E.; Klussmann, M. *J. Org. Chem.* **2014**, *79*, 12033–12040. (c) Mathew, J. S.; Klussmann, M.; Iwamura, H.; Valera, F.; Futran, A.; Emanuelsson, E. A. C.; Blackmond, D. G. *J. Org. Chem.* **2006**, *71*, 4711–4722. (d) Blackmond, D. G. *Angew. Chem., Int. Ed.* **2005**, *44*, 4302–4320. (e) Nielsen, L. P. C.; Stevenson, C. P.; Blackmond, D. G.; Jacobsen, E. N. *J. Am. Chem. Soc.* **2004**, *126*, 1360–1362. (f) Singh, U. K.; Strieter, E. R.; Blackmond, D. G.; Buchwald, S. L. *J. Am. Chem. Soc.* **2002**, *124*, 14104–14114.

(29) Zhao, Y.; Truhlar, D. G. *J. Phys. Chem. A* **2005**, *109*, 5656–5667.

(30) Grimme, S.; Antony, J.; Ehrlich, S.; Krieg, H. *J. Chem. Phys.* **2010**, *132*, 154104.

(31) Klamt, A.; Schüürmann, G. *J. Chem. Soc., Perkin Trans. 2* **1993**, 799–805.

(32) Weigend, F.; Ahlrichs, R. *Phys. Chem. Chem. Phys.* **2005**, *7*, 3297–3305.

(33) Tao, J.; Perdew, J. P.; Staroverov, V. N.; Scuseria, G. E. *Phys. Rev. Lett.* **2003**, *91*, 146401.

(34) Ahlrichs, R.; Armbruster, M. K.; Bär, M.; Baron, H.-P.; Bauernschmitt, R.; Crawford, N.; Deglmann, P.; Ehrig, M.; Eichkorn, K.; Elliott, S.; Furche, F.; Haase, F.; Häser, M.; Hättig, C.; Hellweg, A.; Horn, H.; Huber, C.; Huniar, U.; Kattannek, M.; Kölmel, C.; Kollwitz, M.; May, K.; Nava, P.; Ochsenfeld, C.; Öhm, H.; Patzelt, H.; Rappoport, D.; Rubner, O.; Schäfer, A.; Schneider, U.; Sierka, M.; Treutler, O.; Unterreiner, B.; von Arnim, M.; Weigend, F.; Weis, P.; Weiss, H. *TURBOMOLE v6.5 2013*, University of Karlsruhe and Forschungszentrum Karlsruhe GmbH: Karlsruhe, Germany, 1989–2007; <http://www.turbomole.com>.

(35) Gansäuer, A.; Fleckhaus, A.; Lafont, M. A.; Okkel, A.; Kotsis, K.; Anoop, A.; Neese, F. *J. Am. Chem. Soc.* **2009**, *131*, 16989–16999.

(36) Girard, C.; Kagan, H. B. *Angew. Chem., Int. Ed.* **1998**, *37*, 2922–2959.

(37) Wang, L.-C.; Jang, H.-Y.; Roh, Y.; Lynch, V.; Schultz, A. J.; Wang, X.; Krische, M. J. *J. Am. Chem. Soc.* **2002**, *124*, 9448–9453.